European Journal of Pharmaceutics and Biopharmaceutics 169 (2021) 113–124

Contents lists available at ScienceDirect

European Journal of Pharmaceutics and Biopharmaceutics

journal homepage: www.elsevier.com/locate/ejpb

Preclinical and clinical studies to evaluate cutaneous biodistribution, safety and efficacy of UV filters encapsulated in mesoporous silica SBA-15

André Luis Máximo Daneluti [a], Lucas Offenbecker Guerra [b], Maria Valéria Robles Velasco [a], Jivaldo do Rosário Matos [c], André Rolim Baby [a], Yogeshvar N. Kalia [d,e,*]

[a] Department of Pharmacy, Faculty of Pharmaceutical Sciences, University of São Paulo, Brazil
[b] Allergisa – Investiga Research Institute, Barao Geraldo, Campinas, Sao Paulo, Brazil
[c] Department of Fundamental Chemistry, Institute of Chemistry, University of São Paulo, Brazil
[d] School of Pharmaceutical Sciences, University of Geneva, Switzerland
[e] Institute of Pharmaceutical Sciences of Western Switzerland, University of Geneva, Switzerland

ARTICLE INFO

Keywords:
Mesoporous silica
SBA-15
Avobenzone
Oxybenzone
Octyl methoxycinnamate
Stick incorporated UV filters
Clinical safety
Human skin
Biodistribution
In vivo SPF

ABSTRACT

Innovative technologies have been designed to improve efficacy and safety of chemical UV filters. Encapsulation can enhance efficacy and reduce transdermal permeation and systemic exposure. The aims of this work were (i) to determine the cutaneous biodistribution of avobenzone (AVO), oxybenzone (OXY), and octyl methoxycinnamate (OMC) incorporated in mesoporous silica SBA-15 and (ii) to perform preclinical (*in vitro*) and (iii) clinical safety studies to demonstrate their innocuity and to evaluate sun protection factor (SPF) in humans. Skin penetration studies showed that deposition of OXY and AVO in porcine and human skin after application of stick formulation with incorporated filters (stick incorporated filters) was significantly lower than from a marketed (non-encapsulated) stick. Cutaneous deposition and transdermal permeation of OXY in and across human skin were 3.8-and 13.4- fold lower, respectively, after application of stick entrapped filters. Biodistribution results showed that encapsulation in SBA-15 decreased AVO and OXY penetration reaching porcine and human dermis. Greater deposition (and permeation) of OXY in porcine skin than in human skin, pointed to the role of follicular transport. Stick incorporated filters had good biocompatibility *in vivo* and safety profiles, even under sun-exposed conditions. Entrapment of UV filters improved the SPF by 26% and produced the same SPF profile as a marketed stick. Overall, the results showed that SBA-15 enabled safety and efficacy of UV filters to be increased.

1. Introduction

Ultraviolet (UV) radiation has been linked to several adverse effects, including cutaneous phototoxicity, photoaging and an increased risk of skin cancers [1–3]. The use of formulations containing UV filters can decrease the risk of developing skin carcinoma, actinic keratosis and melanoma [1,4–6]. Chemical organic filters are key sunscreen components that provide protection against skin photodamage by absorbing incident UVA and UVB radiation and then dissipating it as a less harmful energy [7,8].

It is known that the performance of UV filter formulations depends not only on the physicochemical properties of the UV filters, but also on the pharmaceutical excipients used to formulate them into the final product [9]. Therefore, the development of innovative and efficacious sunscreen products is a complex formulation challenge, since appreciable amounts of chemically distinct UV filters must be incorporated into different types of formulations such as emulsions (creams and lotions), oils, alcohols, sticks and powders [9–11].

Organic filters have been challenged due to their photoinstability and possible safety issues. Indeed, the photoreactivity of these compounds can lead to the formation of photoproducts that can absorb in different spectral regions, thus reducing their efficacy [8,12,13]. Regarding safety, there are substantial concerns that organic UV filters could penetrate through the stratum corneum, or via follicles, into epidermal cells, leading to adverse effects such as phototoxicity, allergies and dermatitis dermatitis [14–18]. Moreover, as frequent application and reapplication are recommended, and many of these compounds are present in cosmetics, there is a high risk of systemic absorption. Since sunscreens are applied on large areas of the skin surface, even low penetration rates can cause organic chemical filters to

* Corresponding author at: School of Pharmaceutical Sciences, University of Geneva, CMU – 1 Rue Michel Servet, 1211 Geneva, Switzerland.
E-mail address: yogi.kalia@unige.ch (Y.N. Kalia).

https://doi.org/10.1016/j.ejpb.2021.10.002
Received 28 May 2021; Received in revised form 23 September 2021; Accepted 5 October 2021
Available online 9 October 2021

enter the body in amounts that can cause adverse reactions. As sunscreens must act only on the surface of the skin (stratum corneum), these compounds should not penetrate into the viable epidermis or the dermis and certainly should not pass into the systemic circulation [8,15,18].

Innovative technologies, e.g., encapsulation of UV filters, have been designed to improve the safety and efficacy of chemical filters. A method that can improve UV filter activity, and reduce skin absorption, responsible for toxicity, would be valuable [8,9,19,20]. A number of carrier systems have been widely studied and used in personal care products and topical formulations [9,21–23]. However, topically applied nanocarriers should not permeate across the stratum corneum and reach the viable tissues where they might interfere with biological processes [19]. Despite the scientific data available in the literature on skin penetration and permeation of nanomaterials, there is still a need for comprehensive risk evaluations so that definitive safety profiles related to their effects upon skin exposure can be established [24,25].

Recently, mesoporous silica of type SBA-15 has been used to load molecules inside the pores with high encapsulation/incorporation efficiency, enabling controlled delivery, and increasing compound stability [26–29]. Normally, supramolecular assemblies (copolymer triblock) are required in the synthesis of SBA-15 [28,30,31]. The surfactant will self-aggregate into micelles at a concentration higher than the critical micelle concentration (CMC). Then, the tetraethylorthosilicate (TEOS) – the silica source – can condense at the surface of the micelles forming an inorganic–organic hybrid material. At the end of the process, the template polymer triblock must be removed either by calcination or by solvent extraction to generate pores [30–33]. The resulting silica mesoporous material provides structural and biomedical properties such as ordered porous structure, large pore volume and surface area, tunable particle size and biocompatibility. Several research studies suggest that mesoporous silicas, especially SBA-15, are biocompatible and degrade over time in biological tissue[34,35]. In addition, *in vitro* biocompatibility and cytotoxicity studies of these materials also exhibited low toxicity at low concentrations [31,33,36].

Based on these observations, it was decided to investigate whether UV filters, oxybenzone (OXY), avobenzone (AVO) and octyl methoxycinnamate (OMC)) incorporated into SBA-15 fulfilled safety requirements. In the first part of the study, the preclinical safety *in vitro* and the clinical safety studies in human volunteers, of stick formulation containing incorporated filters (stick incorporated UV filters) and stick formulations containing non-incorporated UV filters (stick non-incorporated UV filters) were assessed. It should be pointed out that "stick" products are frequently used for topical delivery to the skin; their composition is a complex mixture of waxes and oils that are combined to create a product can be spread easily on the skin surface. The second part of the study aimed to evaluate the amount of the UV filters deposited in the skin, the transdermal permeation and to determine the biodistribution of OXY and AVO. Another objective was to compare the biodistribution profiles in human and porcine skins of OXY and AVO after having applied stick incorporated UV filters and a marketed non-encapsulated stick UV filter (marketed stick formulation) and to confirm the suitability of using porcine skin as a surrogate for human skin for these types of studies. Since our previous publication demonstrated that OMC delivery from a stick with non-incorporated filters and stick with incorporated filters was not significantly different [37], it was decided to quantify only OXY and AVO in these skin delivery studies.

2. Materials and methods

2.1. Materials

OXY, OMC, AVO and isopentane were purchased from Sigma-Aldrich (Buchs, Switzerland). Acetone and methanol (all HPLC grade), formic acid, acetonitrile (LC-MS grade) and sodium dodecyl sulfate were purchased from Fisher Scientific (Reinach, Switzerland). Brij® C20 (Cethet 20) was purchased from Croda (Switzerland). Pluronic® P123 poly (ethylene oxide)-poly(propylene oxide)-poly(ethylene oxide) triblock copolymer (EO_{20}-$PO_{70}EO_{20}$) was donated by BASF (Germany), and tetraethylorthosilicate (TEOS) was acquired from Sigma-Aldrich (USA). Ultrapure water (Millipore Milli-Q Gard 1 Purification Pack resistivity > 18 MΩ.cm; Zug, Switzerland) was used to prepare all solutions. All other chemicals were at least of analytical grade.

2.2. SBA-15 preparation and characterization of UV filters into SBA-15

SBA-15 synthesis, the main characterization, morphology results and incorporation of the UV filters in SBA-15 have already been described and published [26,30]. The ordered pore structure of SBA-15 was verified by transmission electron microscopy (TEM) and it was proved that SBA-15 had a symmetrical hexagonal 2D pore distribution [37].

2.3. Incorporation of UV filters into SBA-15

The protocol for incorporation of the UV filters in SBA-15 has been described previously [26]. Briefly, SBA-15 was added to an acetone solution (~100 mL) of the UV filter (AVO, OXY or OMC; OXY (1 g SBA-15: 2 g OXY), AVO (1 g SBA-15: 1 g AVO) and OMC (2 g SBA-15: 1 g OMC). The incorporation process of AVO, OXY and OMC into SBA-15 was evaluated by using nitrogen adsorption isotherm measurements and small angle X-ray scattering (SAXS). The combination of these techniques showed that the UV filters were incorporated into the pores SBA-15. At the same time, it was observed that the mesoporous materials had a hexagonal well-ordered network of regular and cylindrical mesopores [26,37].

2.4. Stick formulations containing the UV filters

Two stick formulations with non-incorporated UV filters and UV filters incorporated in SBA-15 were evaluated [37]. The composition of stick formulations were: Butyl Stearate, Copernicia cerifera (Carnauba) Wax, Ethylene/VA Copolymer, Euphorbia cerifera Wax, Isopropyl Palmitate, Ozokerite, Paraffin, Paraffinum Liquidum, Candelilla wax, Ceresin wax, Cetyl alcohol 20OE, Glyceryl cocoate, Cetyl Acetate, Acetylated Lanolin, Lanolin, Butylene Glycol Cocoate, Castol oil, Propylparaben, BHT and Tocopheryl Acetate. The active ingredients of the formulations is shown in Table 1 [37]. In addition, a marketed sunscreen stick containing "free" UV filters was purchased (Neutrogena®), for comparison with laboratory-prepared stick formulations. The major ingredients of the formulation is: adipic acid/diglycol crosspolymer, beeswax, BHT, C12-15 alkyl benzoate, diethylhexyl 2,6-naphthalate, dimethicone, fragrance, neopentyl glycol diethylhexanoate, neopentyl glycol diisostearate, octyldodecyl neopentanoate, ozokerite, paraffin and polyethylene. The UV filters presented in this formulation are avobenzone (3.0%), homosalate (15.0%), octilsalicilate (5.0%)

Table 1
UV filters and SBA-15 composition (% w/w) of stick formulations.

Composition	Stick formulation codes (concentration %, w/w)		
	Stick + SBA-15	Stick non-incorporated filters	Stick incorporated filters
Ethylhexyl Methoxycinnamate (octyl methoxycinnamate)*	–	5.0	–
Butyl methoxydibenzoylmethane (avobenzone)*	–	3.0	–
Benzophenone-3 (oxybenzone)*	–	4.0	–
SBA-15	15.0	–	–
SBA-15/OMC (2:1) **	–	–	15.0
SBA-15/AVO (1:1) **	–	–	6.0
SBA-15/OXY (1:2) **	–	–	6.0

* Free UV filters.
** Concentration in % corresponding to free UV filters [37].

(reported to be a penetration enhancer), otocrylene (10.0%), oxybenzone – benzofenona-3 (3.0%).

2.5. Quantification of UV filters

2.5.1. Quantification of AVO and OXY by HPLC-UV

HPLC-UV was used in order to quantify UV filters in the stick formulations using a previously published method [37]. HPLC apparatus consisted of a P680A LPG-4 pump equipped with an ASI-100 autosampler, a thermostatted column compartment TCC-100, and a UV170U detector (Dionex; Voisins LeBretonneux, France). UV filters were assayed using a detection wavelength of 238 nm. Gradient separation was performed using a LiChrospher®100, RP-18e, 5 μm, 125 × 40 mm column (BGB Analytik AG; Boeckten, Switzerland) which was maintained at 20 °C. Chromeleon™ software was used for integration and data analysis. The flow rate and injection volume were 1.0 mL min^{-1} and 20 μL, respectively. The mobile phase consisted of a mixture of methanol and water (85:15 v/v). OXY, AVO and OMC eluted at 5.4, 15.0 and 16.7 min, respectively; and the run time was 20 min [38,39]. The limits of detection (LOD) and quantification (LOQ) for OXY, AVO and OMC were 0.3, 1.8 and 1.2 μg mL^{-1} and 2.5, 7.5 and 5.0 μg mL^{-1}, respectively. The HPLC-UV method was validated as per ICH guidelines. Complete details are given in the Supplementary Information.

Three sample replicates of each formulation were prepared as follows: 15.0 mg of each stick sample was transferred into a 10 mL volumetric flask and diluted to volume with methanol, followed by an ultrasonic bath treatment for 30 min. After filtration through a Millipore filter membrane with a pore size of 0.45 μm, 20 μL of each sample solution and standard solution were injected in the HPLC [37,40]. The amounts of OXY, AVO and OMC in the formulations were: – non-incorporated stick formulation – 3.8, 3.3 and 4.5, and incorporated UV filters formulation – 3.5, 2.7 and 6.0 %, respectively [37].

2.5.2. Quantification of AVO and OXY by UHPLC-MS/MS

Skin deposition and transdermal permeation of AVO and OXY and their cutaneous biodistribution were determined using UHPLC coupled with tandem mass spectrometry, using a previously described and validated method [37].

UHPLC-MS/MS analysis was carried out using a Waters Acquity® UPLC® system (Baden-Dättwil, Switzerland) comprising a binary solvent pump, a sample manager, and a Waters XEVO® TQ-S Micro tandem quadrupole detector (Baden-Dättwil, Switzerland). Gradient separation was performed with a Waters XBridge® BEH RP-C18, 2.1 × 50 mm column containing 2.5 μm particles and thermostatted at 20 °C, and the mobile phase comprised a mixture of Milli-Q water and ACN both containing 0.1% formic acid. A flow rate of 0.2 mL min^{-1} and an injection volume of 5 μL were used. AVO and OXY were detected with electrospray ionization in positive ion mode using multiple reaction monitoring (MRM). The lower limits of detection (LOD) and quantification (LOQ) for all UV filters were 3.0 ng mL^{-1} and 10.0 ng mL^{-1}, respectively [37] (Supplementary Information).

2.6. Skin source and preparation

2.6.1. Porcine skin

Porcine ears were obtained from a local slaughterhouse (CARRE; Rolle, Switzerland). The skin samples were harvested from the underlying tissue using a scalpel. Hair was carefully trimmed using clippers to avoid damage to the skin. The excised skin samples (thickness ~1.0 mm) were then punched out (Berg & Schmid HK 500; Urdorf, Switzerland) and stored at −20 °C and stored for a maximum period of 3 months.

2.6.2. Human skin

Human skin samples were collected immediately after surgery from the Department of Plastic, Aesthetic and Reconstructive Surgery, Geneva University Hospital (Geneva, Switzerland). The study was approved by the Central Committee for Ethics in Research (CER: 08-150 (NAC08-051); Geneva University Hospital). The hypodermis and fatty tissue were removed and skin samples were punched out into 32 mm circular disks. The skin discs were subsequently horizontally sliced with a Thomas Stadie-Riggs slicer (Thomas Scientific; Swedesboro, NJ, US) to obtain a thickness of ~1 mm. The skin was stored in a biobank at −20 °C for a maximum period of 3 months.

2.7. Evaluation of AVO and OXY skin delivery in vitro

Skin samples (porcine or human) were mounted on standard Franz diffusion cells (area = 2 cm^2). The receptor compartment (volume = 11 mL) was filled with sonicated phosphate buffered saline (PBS, pH 7.4) containing 0.5% Brij® C20 to maintain sink conditions [37,41]. After equilibration, approximately 11.5 mg (5.70 ± 0.20 mg cm^{-2}) of marketed stick formulation and stick formulation with incorporated filters were applied to the donor compartment. The receiver phase was stirred at 400 rpm and maintained at 33 °C throughout the experiment for 12 h [37]. The amounts of OXY (3.0%) and AVO (3.0%) applied from the marketed stick were: 170 μg cm^{-2}, for both compounds. For the stick with incorporated filters, the amounts of OXY (3.5%) and AVO (2.7%) applied were 200 and 150 μg cm^{-2}, respectively. After 12 h, a 1 mL aliquot was withdrawn from the receiver compartment to quantify AVO and OXY permeation across the skin. Samples were centrifuged at 10 000 rpm for 15 min and analyzed by UHPLC-MS/MS. The diffusion cells were dismantled, and each sample was carefully cleaned by the application of a cotton swab imbibed with 1.0% (w/w) aqueous solution of sodium dodecyl sulfate in order to mimic human skin cleansing with a liquid soap [37]. AVO and OXY deposited in the skin was extracted by cutting the skin samples into small pieces and soaking in 4 mL of acetonitrile overnight with continuous stirring at room temperature. The extraction samples were centrifuged at 10 000 rpm for 15 min and diluted (if required) prior to UHPLC-MS/MS analysis [37].

2.8. Determination of the OXY and AVO biodistribution profile in porcine and human skin

The stick incorporated formulation and the marketed stick were applied for 12 h to the porcine and human skins samples with a spatula using the conditions described above (n = 5). Once the experiment was terminated, a small area of 1.2 cm^2 was punched out from the 2 cm^2 skin samples. These skin samples were snap-frozen in isopentane cooled to its freezing point (−160 °C) with liquid nitrogen and mounted in a cryotome (Microm HM 560 Cryostat, Walldorf, Germany) so as to obtain horizontal (XY-plane) lamellae; there were 2 lamellae with a thickness of 20 μm and 19 lamellae with a thickness of 40 μm. A total of 21 lamellae was taken from each sample - going from the skin surface to a depth of 800 μm, providing tissue samples from the stratum corneum, viable epidermis, and dermis. Each slice was collected in an individual Eppendorf tube. The UV filters deposited in each slice were extracted overnight with 200 μL of acetonitrile under stirring at room temperature. Each extract was subsequently subjected to UHPLC-MS/MS analysis [37,41].

2.9. Pre-clinical – in vitro – measures of irritation potential

HET-CAM (hen's egg test-chorioallantoic membrane) was used to evaluate the irritation potential of SBA-15 and the incorporated UV filters (AVO, OXY and OMC) into SBA-15. Chicken eggs were kept in an incubator equipped with an automatic rotation device for 9 days at 37 °C and 65% relative humidity [23,42,43]. After incubation, eggs were opened and the shell membrane was hydrated with 300 μL of 0.9% NaCl solution. The same volume of diluted stick formulations (stick contained SBA-15 (blank) and incorporated stick formulation) into caprylic/capric triglyceride was applied on the chorioallantoic membrane (at concentration of 0.05 g mL^{-1}). The positive control used was sodium dodecyl

sulfate (SDS) solution (1.0%) (for vascular hemorrhage and lysis), while the negative control was NaCl solution (0.9%) [23,42–44]. The assay was carried out in triplicate and monitored until the appearance of the vascular events (hemorrhage, lysis and coagulation) for 5 min and the onset time of these three events was recorded. The irritation scores were calculated as described in Eq. (1) [23,44,45]

$$IS = \frac{(301 - H)5 + (301 - L)7 + (301 - C)9}{300} \quad (1)$$

where IS: irritation score; H: onset time in seconds for start of hemorrhage; L: onset time in seconds for start of lysis; C: onset time in seconds for start of coagulation. The materials tested were classified according to irritancy score: 0–0.9 = non-irritant; 1–4.9 = slight irritant; 5–8.9 = moderate irritant; 9–21 = strong irritant.

2.10. Clinical studies in human volunteers

The *in vivo* tests were conducted by Alergisa (Campinas-SP, Brazil). The experiments were conducted in accordance with the ethical standards of the committee on human experimentation of the *Investiga Research Institute Ethics Committee* (SPF *in vivo* - CAAE 94422418.0.0000.5599; process number 2.802.494; Human repeat insult patch test and Photo irritation and photosensitivity potential - CAAE 94420418.1.0000.5599; process number 2.802.501) and with the Declaration of Helsinki Principles. Informed oral/written consent for the safety and efficacy tests was obtained for all participants (subjects). Stick non-incorporated filters, stick with incorporated filters and marketed stick were evaluated, as well as a standard sample.

2.10.1. Human repeat insult patch test – HRIPT

The six-week cutaneous compatibility experiment was conducted in 58 male and female volunteers, after oral informed and written consent were obtained. The volunteers were 18–68 years old and had skin phototypes II–IV. Stick formulations and saline solution (negative control) were applied using occlusive patches on the backs of volunteers for 48 h, three times a week. The skin was scored 30 min later, and new material was applied for two more weeks. The next two weeks were characterized as a rest period, no samples were applied. After this period, fresh patches with the samples were applied for one last week, the challenge phase. The scores used were 0 for no erythema, 1 for well-defined erythema, 2 for erythema and induration, and 3 for vesiculation and bullous reaction [1,19,46–48].

2.10.2. Photo-irritation and photosensitivity potential

The photo-irritation and photosensitivity (six weeks) potential experiments were performed in 33 male and female volunteers aged between 26 and 70 years old and with skin phototypes II and III. The photo irritation experiment was performed in order to evaluate the absence of irritant potential of a product applied to the skin when exposed to UVA radiation [1]. Epicutaneous patches were applied to the backs of volunteers, under occlusion with 0.05 g cm^{-2} of the stick formulations and the negative control (NaCl 0.9%). After 24 h, the patch was removed and the application sites were evaluated and submitted to artificial UVA irradiation, with irradiance of 10.5 mW cm^{-2} and dose of 6 J cm^{-2} (equivalent to an exposure time of 6 min and 40 s). After 24 h, the volunteer's skin was once more evaluated for possible irritation reactions induced by UVA radiation [1,49,50].

The evaluation of the photosensitivity potential consisted of three phases: induction, rest and challenge. The experiment was performed simultaneously with the photo irritation test, using the same participants and samples. A three-week induction period was performed, where the formulations and the negative control were applied under occlusion on the backs of the participants, twice per week. After 24 h of each application, the patch was removed and the application sites were evaluated and submitted to artificial UVA irradiation with irradiance of 10.6 mW cm^{-2} and dose of 6.3 J cm^{-2}. After the induction period, the volunteers entered the resting period, lasting for 10 days (no samples were applied to the participants). After that, the challenge period started and a new patch containing the samples and the negative control was applied to the back of the volunteers, in an area where no patch had been previously applied. After 24 h, the patch was removed and the areas were evaluated and subjected to UVA radiation with the same specifications used in the induction phase. Finally, after 24 h of the irradiation, the areas related to the challenge test were evaluated in relation to possible reactions of photosensitization[1,49,50]. The scores employed were: 0 for no erythema, 1 for well-defined erythema, 2 for erythema and induration, and 3 for vesiculation and bullous reaction [1,19,48,51].

2.10.3. In vivo SPF and in vitro UVA-PF

The three stick formulations (with non-incorporated filters, incorporated filters and the marketed stick) were analyzed for the SPF and UVA-PF parameters. *In vivo* SPF experiment was conducted according to a well-established method [52]. The experiment was performed in 10 healthy subjects with Fitzpatrick skin types II or III. An amount of 2.0 mg cm^{-2} was applied to each participant, and a Multiport® 601 (Solar Light Company) solar UV simulator was employed. SPF value was defined as the UV energy required to produce a minimum erythemal dose (MED) on protected skin, divided by the UV energy required to produce a MED on unprotected skin (Eq. (2)) [23]. The standard sample was the reference sunscreen formulation (SPF = 16.3) [1,23,48,52].

$$SPF = \frac{MED\ of\ protected\ skin}{MED\ of\ unprotected\ skin} \quad (2)$$

In vitro UVA-PF and critical wavelength determination was carried out according to the determination of the UVA protection factor and critical wavelength guideline [53]. Four PMMA plates were prepared for each product to be tested and 9 measures were performed on each plate. Transmission measurements between 290 and 400 nm were carried out using a spectrophotometer equipped with an integrating sphere (UV transmittance analyzer UV1000S, Labsphere, North Sutton, US) [1,23,48]. The coefficient of the variation for the individual UVA-PF values after irradiation was evaluated and did not exceed 20%.

2.11. Statistical analysis

Data were expressed as the mean ± SD. Outliers determined using the Dixon test were discarded. Results were evaluated statistically using analysis of variance (ANOVA) one-way followed by the Tukey test for multiple comparisons and Student's *t* test. The level of significance was fixed at $\alpha = 0.05$.

3. Results and discussion

3.1. Evaluation of AVO and OXY skin penetration in vitro

In this experiment the marketed stick containing non-incorporated UV filters and the stick with incorporated filters were used. The optimal exposure time of 12 h was selected according to the results of the previous study [37]. No AVO was detected in the receptor compartment after application of any of the stick formulations for 12 h. For OXY, the permeation results for both formulations (marketed stick and formulation with incorporated filters) showed that this UV filter was present in the receptor compartment. However, the amount of OXY from stick formulation with incorporated filters was > 10-fold lower ($p < 0.05$) than that from the marketed stick for both porcine (151 ± 47 vs 2020 ± 630 ng cm^{-2}) and human (79 ± 55 vs 1292 ± 200 ng cm^{-2}) skins (Fig. 1).

The comparison between porcine and human skins demonstrated that the amount of OXY permeated from the stick with incorporated filters was equivalent ($p > 0.05$), although the OXY amount permeated

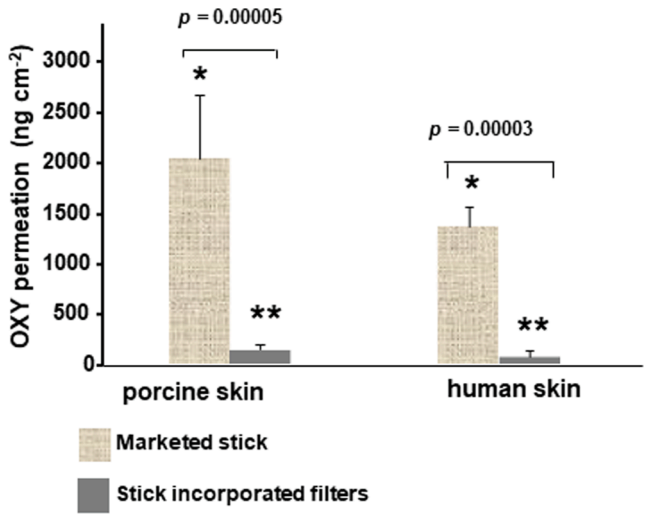

Fig. 1. Comparison of OXY skin permeation in full-thickness porcine and human skin after 12 h application of marketed stick and stick incorporated filters (means ± SD; n = 8). Comparison marketed stick between porcine and human skins (*p = 0.00003); Comparison stick incorporated filters between porcine and human skins **p = 0.36380).

from the marketed stick formulation was greater in porcine skin than in human skin ($p < 0.05$). In addition, OXY deposition from the stick with incorporated filters was significantly lower than that from the marketed formulation for both porcine (12.0 ± 2.6 vs 3.0 μg cm^2 ± 1.0) and human (6.5 ± 2.5 vs 1.8 ± 0.7 μg cm^2) skins (Fig. 2a). The amount of AVO delivered to porcine and human skins from the stick with incorporated filters (Fig. 2b) (2.2 ± 0.4 μg cm^2 and 1.2 ± 0.4 μg cm^2, respectively) was lower than that from the marketed stick (6.8 ± 3.0 μg cm^2 and 2.4 ± 1.0 μg cm^2, respectively).

As can be seen from Fig. 1, OXY permeation from the stick formulation with incorporated filters was 16.4 and 13.4-fold lower than that from the marketed stick formulation in human and porcine skins, respectively. In addition, the stick formulation with incorporated filters showed a 4-fold decrease in the amount of OXY present in porcine skin and a 3.8-fold reduction with human skin (Fig. 2a). In the case of AVO (Fig. 2b), a significant reduction was observed in the amount in porcine (3-fold) and human (2-fold) skins as compared to that from the marketed stick formulation. These results demonstrated that SBA-15 was able to reduce the cutaneous penetration (AVO and OXY) and transdermal permeation of UV filters (OXY) in porcine and human skins. Therefore, it suggested that systemic exposure of both filters would be much reduced and even avoided.

Skin penetration of OXY and AVO from both formulations was greater in porcine skin than in human (Fig. 2 a and b). In the case of the marketed stick, OXY and AVO deposition in porcine were 1.8-fold (OXY) and 2.6 fold (AVO) higher than in human skin; whereas for the stick incorporated formulation, the amount of OXY and AVO delivered to porcine skin were 1.7-fold and 1.8-fold higher than in human skin, respectively (See below).

3.2. *Determination of the OXY and AVO biodistribution profile in porcine and human skins*

The biodistribution profiles of OXY (Fig. 3 a and b) and AVO (Fig. 4 a and b) in porcine and human skins showed that skin deposition from the stick incorporated filters was significantly lower than that from the marketed stick in both the upper 160 μm and in the deeper (320 – 800 μm) skin layers ($p < 0.05$). OXY deposition from the stick incorporated filters down to the total depth (800 μm) was significantly lower than that from the marketed stick for both porcine (1448.7 ± 499.4 ng cm^{-2} vs 5612.3 ± 642.9 ng cm^{-2}) and human skin (482.4 ± 113.9 ng cm^{-2} vs

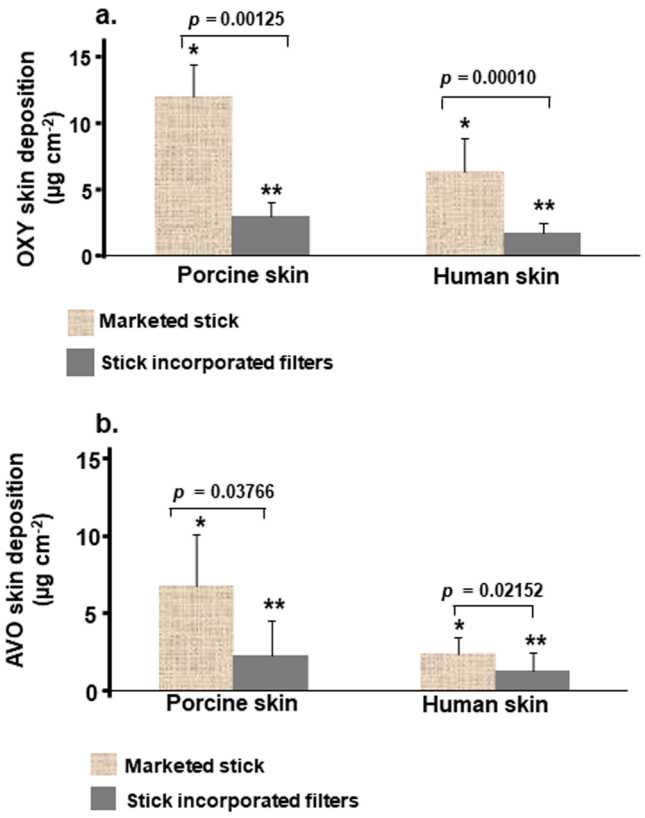

Fig. 2. (a). Comparison of OXY deposition in in full-thickness porcine and human skin after 12 h application of marketed stick and stick incorporated filters (means ± SD; n = 8). Comparison marketed stick formulation between porcine and human skins (*p = 0.00922); Comparison stick incorporated filters between porcine and human skins (**p = 0.01204), Fig. 2. (b). Comparison of AVO deposition in in full-thickness porcine and human skins after 12 h application marketed stick and stick incorporated filters (means ± SD; n = 5). Comparison marketed stick between porcine and human skins (*p = 0.03931); Comparison stick incorporated filters between porcine and human skins (**p = 0.01347).

3917.9 ± 698.4 ng cm^{-2}) (Fig. 3 a and b), whereas the amounts of AVO deposited (Fig. 4a and b) from stick incorporated filters were 1.7-(human skin) and 3-fold (porcine skin) (440.5 ± 57.6 ng cm^{-2} and 448.2 ± 217.2 ng cm^{-2}, respectively) lower than the marketed stick (753.5 ± 102.7 ng cm^{-2} and 1400.8 ± 559.5 ng cm^{-2}, respectively)[37].

Quantification of AVO and OXY in the individual 20 and 40 μm thick lamellae after application of stick formulations enabled the detailed evaluation of their deposition as a function of depth and the anatomical regions. Fig. 3c and d and Fig. 4c and d present the OXY and AVO deposition in the different layers of porcine and human skin, after application of stick formulations (stratum corneum: 0–40 μm; viable epidermis 40–160 μm; dermis 160–800 μm) [37,41,54].

The stick incorporated filters yielded significantly lower accumulation of OXY (Fig. 3c and d) in the stratum corneum, viable epidermis and dermis, reducing filter deposition 2.5, 2.8- and 5-fold, respectively, while for human skin, the deposition of OXY in stratum corneum, viable epidermis and dermis decreased by 3.4-, 7.7- and 11-fold, respectively. A study performed by Marcato et al[55] on the ability of poly(caprolactone) (PCL) nanoparticles to reduce OXY delivery to human skin demonstrated similar skin deposition. After 24 h, the authors observed that the encapsulation of OXY significantly reduced skin deposition to epidermis (3.7-fold) and dermis (3-fold) than formulation containing the non-encapsulated filter.

In addition, the incorporation process of AVO decreased the amounts

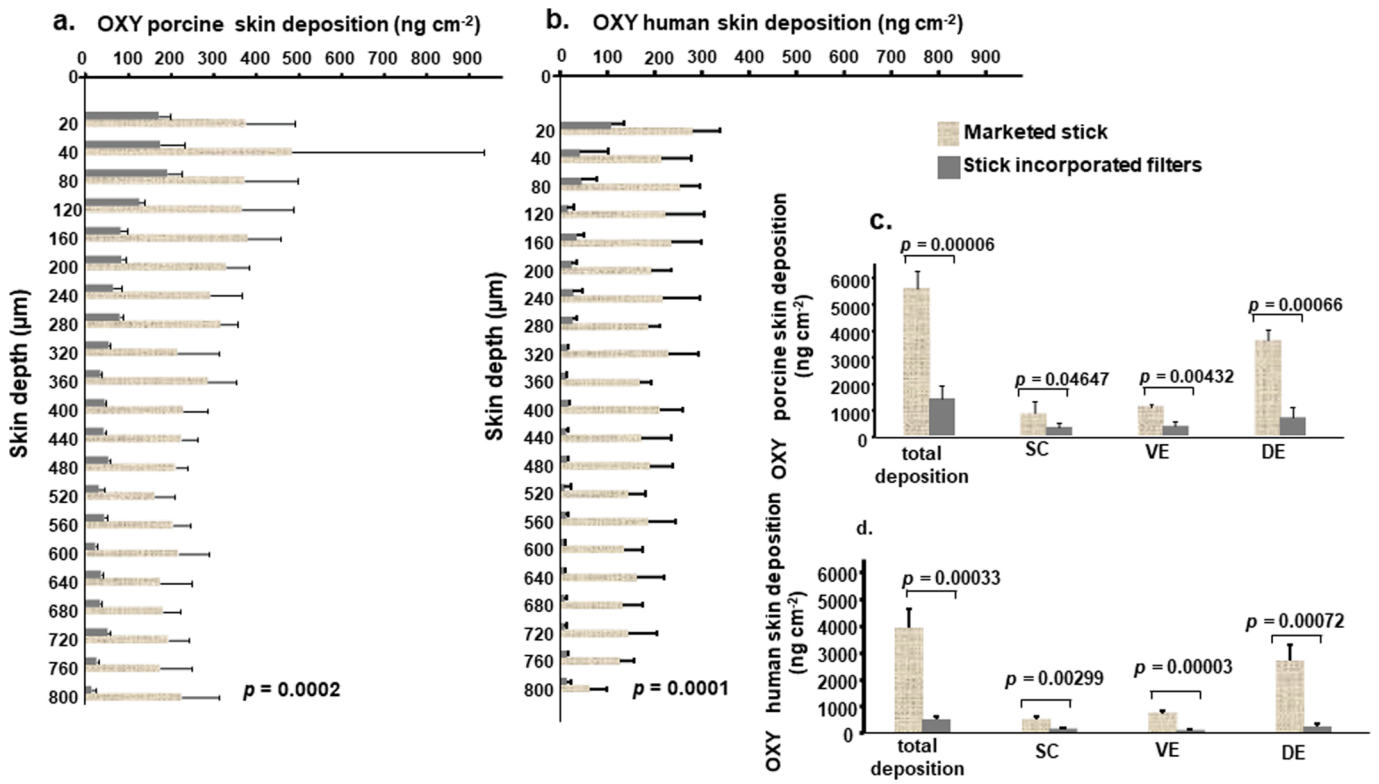

Fig. 3. Cutaneous biodistribution profile of OXY in the layers of porcine (a) and human (b) skins (stratum corneum, viable epidermis and dermis – to total depth of 800 µm and at a resolution of 20 and 40 µm) following a 12 h application of marketed stick and stick incorporated filters. OXY deposition in the layers of porcine (c) and human (d) skins (stratum corneum, viable epidermis and dermis, to total depth of 800 µm) following application a 12 h of marketed stick and stick incorporated filters (means ± SD; n = 5; test-t p $^{<}$0.05). SC = stratum corneum; VE = viable epidermis and DE = dermis.

in viable epidermis and dermis from porcine skin (Fig. 4 c and d), whereas for human skin a significant reduction was observed in stratum corneum and dermis ($p < 0.05$). This was again consistent with earlier work by Puglia et al. [9] where lipid nanostructures of AVO were applied to human epidermis for 24 h, and it was found that they drastically reduced AVO skin permeation, since it was retained mainly on the skin surface.

Regarding the comparative biodistribution study between porcine and human skins, it was demonstrated that the amount of OXY deposited in stratum corneum, viable epidermis and dermis, (Fig. 5 a and b) from both formulations was significantly higher in porcine skin than in human skin ($p < 0.05$), while for AVO, deposition (Fig. 6 a and b) from incorporated stick formulation was not significantly different between human and porcine skins ($p > 0.05$).

Porcine skin is considered as one of the best surrogates for human skin, due to its similarity in terms of thickness and epidermal composition, dermal structure, lipid content and overall morphology [54,56,57]. Nevertheless, it is well known that human skin is the ideal choice for *in vitro* permeation studies, mimicking the real use conditions of photoprotector formulations [56,58]. In contrast to drug delivery studies where the main objective is to ensure that the surrogate does not overestimate delivery and hence therapeutic efficacy, the aim here was to see whether the results with porcine and human skin were consistent and there was no significant overestimation of cutaneous penetration and eventual risk of systemic exposure. The results demonstrated that OXY and AVO total deposition from both formulations yielded slightly greater "delivery" to porcine skin. In addition, OXY deposition into stratum corneum (1.7-fold), viable epidermis (2.8-fold) and dermis (1.3-fold) was also greater than that in human skin for both formulations (Fig. 5a and b). AVO deposition in all skin layers was not different between porcine and human skins upon application of the incorporated stick (Fig. 6a and b) ($p > 0.05$); however, the amount of AVO delivered from the marketed stick formulation was significantly lower in human skin (epidermis: 2.4-fold lower and dermis: 2.6-fold lower) than in porcine skin. These experiments were performed with human skin samples from abdominoplasty patients; thus, skin presented only small vellus hair follicles whereas hair in porcine skin is similar to morphology of larger terminal hairs [57,59]. Furthermore, hair follicles in pig ears can extend up to 1.2 mm into dermis, whereas human hair follicles penetrate far less into this layer [57,60]. Skin penetration of chemical compounds can occur via a "transepidermal route", i.e. via the intercellular lipid space, or through a "trans-appendageal route", utilizing the sweat glands and across the hair follicles associated with the sebaceous glands as shunt pathways. The trans-appendageal structures presents a small percentage of the skin surface area but their importance depends on the permeant's physicochemical characteristics and whether it is free to diffuse or whether it is encapsulated in a much larger carrier system [15,61–63]. Lademann et al. [64] performed a comparative study between human skin (*in vivo* conditions) and porcine skin *in vitro* by following application of sunscreen formulation containing octyl methoxycinnamate. After one hour, the stratum corneum was removed by tape stripping and the amount of this filter was quantified by UV/VIS spectrophotometry. It was demonstrated that the deposition of octyl methoxycinnamate was not significant for both skins. These results might be explained due to the short exposure time of the formulation and as well as the human skin under *in vivo* conditions has slightly difference compared with *ex vivo* human tissue. In spite of these results, the authors assumed that some porcine skin samples present a slightly deeper penetration than human skin, which can be explained due to the larger orifices of the porcine hair follicles.

The incorporated stick demonstrated a significantly reduction in the total deposition of OXY and AVO in human and porcine skins. These findings are consistent with the biodistribution profile of both compounds, which can be evidenced by the decrease in the amount of OXY

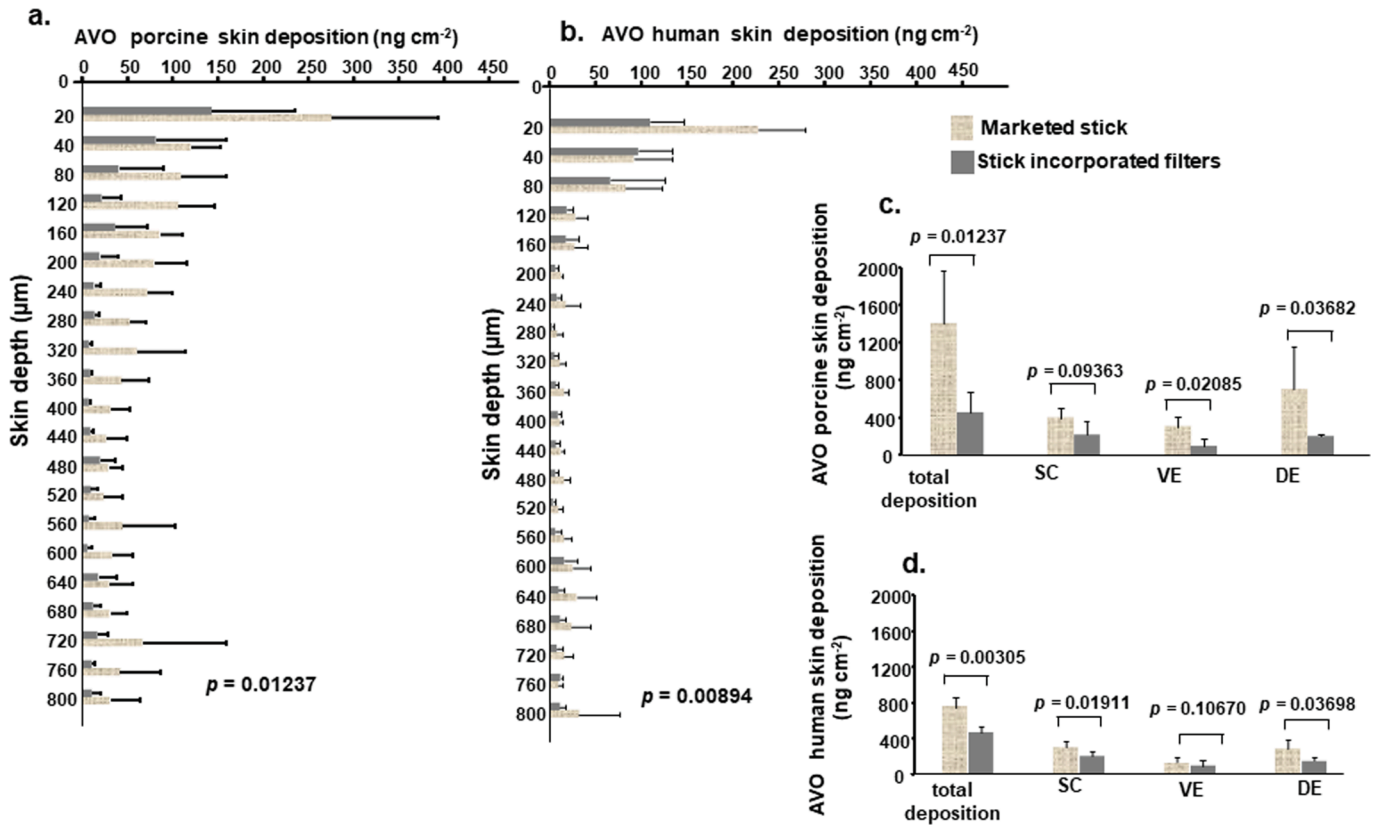

Fig. 4. Cutaneous biodistribution profile of AVO in the layers of porcine (a) and human (b) skins (stratum corneum, viable epidermis and dermis – to total depth of 800 µm and at a resolution of 20 and 40 µm) following a 12 h application of marketed stick and stick incorporated filters. AVO deposition in the layers of porcine (c) and human (d) skins (stratum corneum, viable epidermis and dermis, to total depth of 800 µm) following application a 12 h of marketed stick and stick incorporated filters (means ± SD; n = 5 ; test-t $p < 0.05$). SC = stratum corneum; VE = viable epidermis and DE = dermis.

and AVO delivered into deep layers of human and porcine skins (dermis), bringing further evidence that the physicochemical interaction between SBA-15 and UV filters might decrease the release and diffusion of AVO and OXY [37].

3.3. Irritant potential assay

The HET-CAM is considered to be a rapid, sensitive and inexpensive *in vitro* method for predicting the eye irritant effect of chemical products [65]. In addition, HET-CAM is a validated method that presents comparable results to the Draize test, which is performed on rabbits and is currently not recommended for testing raw materials or cosmetic products, especially for highly irritating or corrosive substances [65–68]. The irritant scores of the tested stick formulations, and the positive (SDS and NaOH) and negative (NaCl) controls are given in Table 2.

Both positive controls induced hemorrhage and lysis, in a few seconds (~20 s) for SDS, while for NaOH a coagulation phenomenon was observed (~40 s); therefore, they were classified as strong irritants. The negative control (0.9% NaCl) did not cause any vascular events. Based on the irritant scores, both formulations (stick blank and stick incorporated filters) were classified as non-irritants, since no vascular events were observed [45]. The images shown in Fig. 7 confirmed that the formulations did not promote hemorrhage, lysis or coagulation events.

Safety studies are mandatory for nanomaterials and dermatological compounds, therefore, the irritation potential test might be a preventive solution and convenient option for preclinical safety experiments [69]. The HET-CAM is considered a reliable assay to track the non-irritating potential of chemical compounds, cosmetics and nanostructured materials [23,67]. The selection of this method was relevant for this research since stick formulations are intended to be applied to the face. During application, the users might apply it near the eye area and may cause ocular irritancy. Thus, HET-CAM results demonstrated that formulations containing SBA-15 and incorporated UV filters had no potential to cause ocular irritation.

3.4. Clinical studies

3.4.1. Evaluation of clinical safety and irritation potential

As shown in Table 3, the clinical safety analysis demonstrated that the three stick formulations had good performance with respect to skin compatibility, phototoxicity and photosensitivity assays. After 24 h or repeated application of stick formulations, no erythema nor edema events were detected, when these formulations were compared with the negative control.

The clinical studies performed here demonstrated that the stick formulation containing filters incorporated in SBA-15 presented a safe profile under extreme use and sun exposure conditions. When testing this formulation under occlusion and during a long time period, it did not lead to any skin irritation or allergic reactions. In addition, incorporation of UV filters into SBA-15 did not present phototoxicity nor photosensitivity. Stick formulations contain highly lipophilic components, waxes and emollients, which in general are classified as low irritation ingredients [37,67]. SBA-15 is synthesized using a non-ionic triblock copolymer (Pluronic® P123) that acts as a structure-directing template [30,70]. During the synthesis of this material, it is necessary remove the triblock copolymer that was used. In general, the total removal of this material is performed by calcination [27,28]. Several *in vivo* and *in vitro* studies have demonstrated that the presence of the triblock copolymer increases the toxicity of SBA-15 [33,35,71]. For this

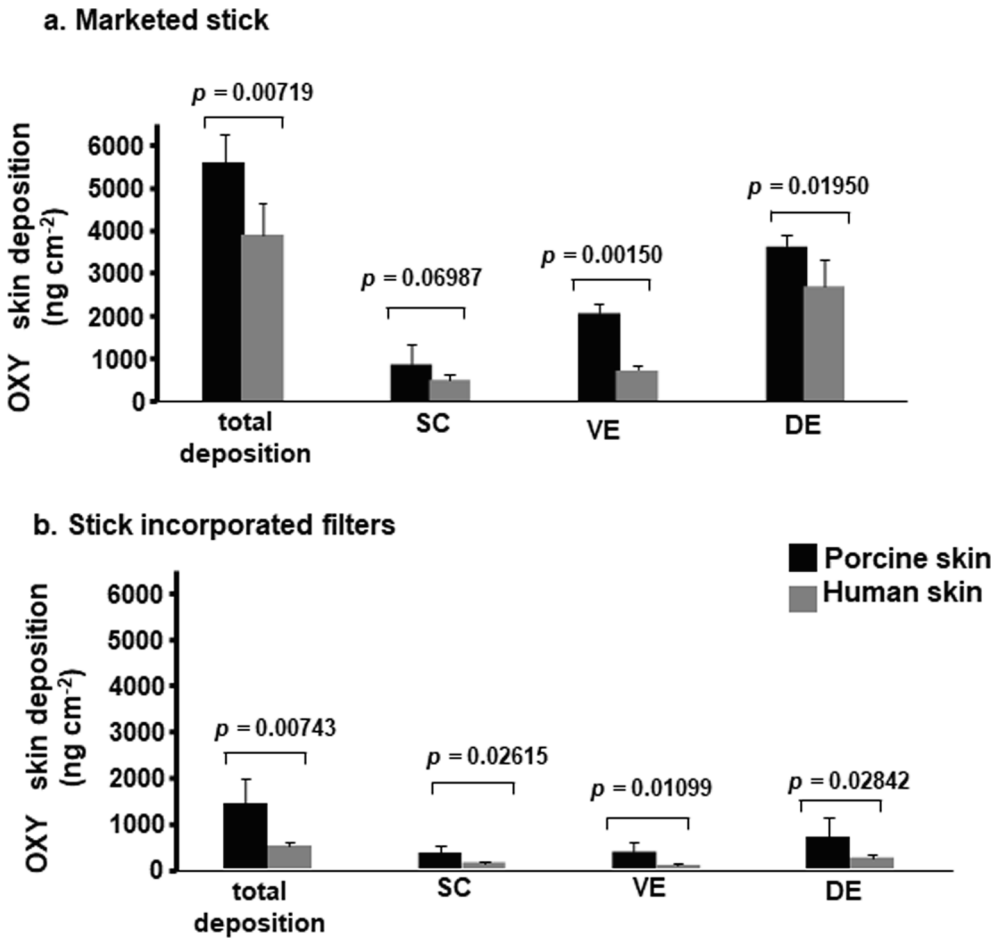

Fig. 5. Comparison of OXY deposition in the upper layers of porcine and human skin (stratum corneum, viable epidermis, and dermis – to a total depth 800 μm) following a 12 h application of marketed stick (a) and stick incorporated filters (b) (means ± SD; n = 5 porcine skin, n = 4 human skin; test-t $p < 0.05$). SC = stratum corneum; VE = viable epidermis and DE = dermis.

reason, the removal of this surfactant makes the SBA-15 a safe and low toxicity material for topical use. These findings were in accordance with irritant potential assay results, which demonstrated that SBA-15 did not cause irritation.

3.4.2. In vivo SPF and in vitro UVA-PF studies

Studies have been performed to compare *in vitro* and *in vivo* assays used to evaluate sun protection factor (SPF) [1,23]. Previous studies conducted by our group demonstrated that incorporated UV filters significantly increased the SPF values in comparison to non-encapsulated UV filters [37]. Moreover, the *in vitro* SPF results (Table 4) showed that the incorporation process increased the efficacy of UV filters (179.3) as compared to the marketed stick products (142.2) and stick with free UV filters (94.3) [37].

Table 5 describes the *in vivo* SPF and *in vitro* UVA-PF results. SPF values showed that all stick formulations were classified as sunscreens, considering that the SPF values were >6 (SPF ≥ 6). In addition, all stick formulations achieved critical wavelength (>370 nm). Regarding the UVA-PF results, it was demonstrated that the level of UVA-PF obtained for all samples was <1/3 of the SPF value [53,69]. To register sunscreen products in the market, current regulation requires labelling of products documenting clinical studies of *in vivo* SPF and *in vivo* or *in vitro* UVA-PF [28]. Nowadays, UVA-PF *in vitro* methods have replaced *in vivo* methods since they are considered fast and inexpensive, while presenting a good correlation with *in vivo* experiments [72,73]. However, some authors have argued that during the assessment of *in vitro* experiments thin films of products, the optical properties of sunscreen formulations might be influenced by several factors, such as uniformity of the film and, possibly, in the case of cosmetic/make-up products containing sunscreens, the presence of highly lipophilic excipients and pigments [72,74]. Since stick formulations prepared here presented only lipophilic components, it is difficult to reach a uniform film in the PMMA plate and therefore decreasing the *in vitro* UVA performance [37,74]. Another explanation might be linked to the fact that the combination of OXY (UVA/UVB filter) and AVO (UVA filter) was not able to improve UVA profile of the formulation.

The stick containing incorporated filters produced a higher SPF value than the non-incorporated stick. The SPF value was enhanced by 26% when UV filters were incorporated into SBA-15 (from 50.4 ± 10.2 to 63.7 ± 10.1). However, the SPF values of the stick incorporated filters and the marketed stick were similar. This was probably due to the combination of three types of UVB absorbers (homosalate, octylsalate, and octocrylene) in the composition of the marketed formulation, which contributed to increasing its SPF [75]. Nevertheless, it is important to emphasize that despite only one UVB absorber filter (OMC) and UVA/UVB filter (OXY) were used, the incorporated stick formulation (63.7 ± 10.1) produced a similar SPF to the marketed stick formulation (69.5 ± 14.4).

Several nanostructured materials and systems have already been investigated in order to increase photoprotection of UV filters and to reduce the concentrations of these chemicals in the sunscreen formulations [14,23]. However, only a few SPF studies *in vivo* have been performed with encapsulated/incorporated UV filters [19], most investigations were performed *in vitro* [4,8,76,77].

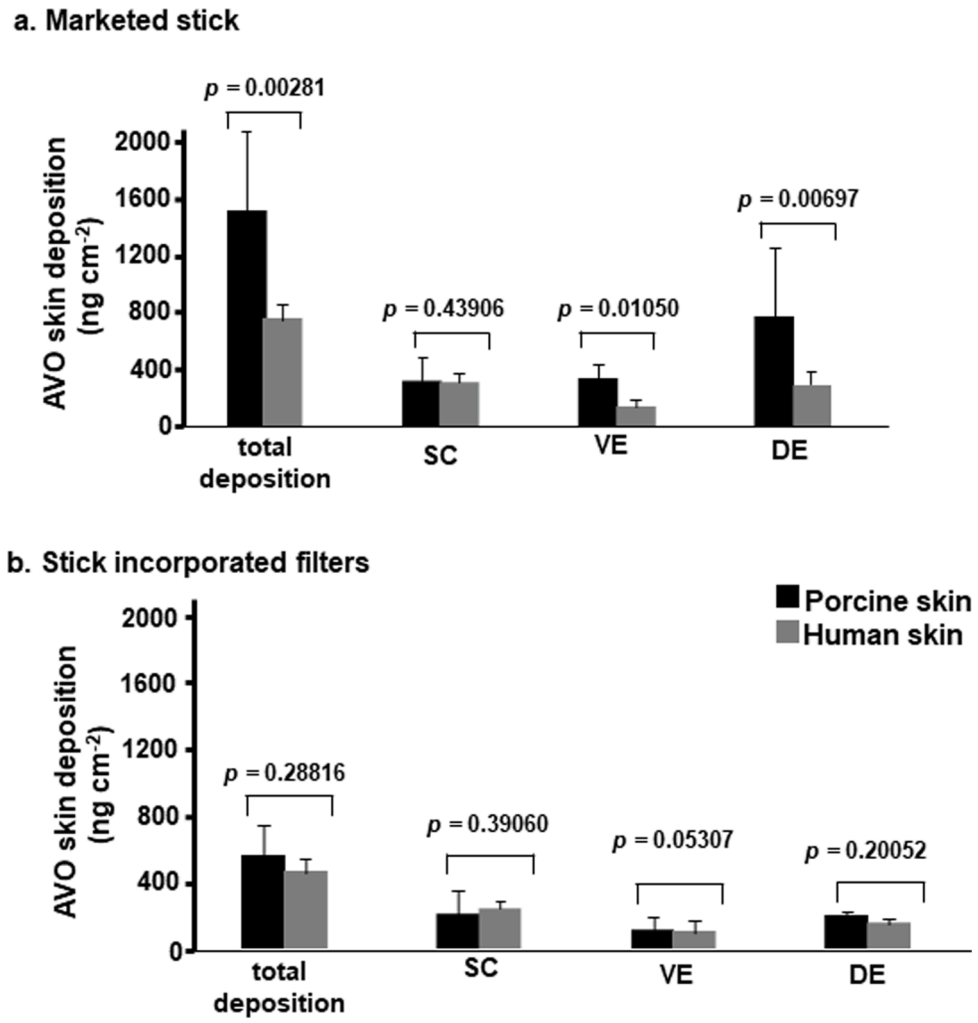

Fig. 6. Comparison of AVO deposition in the upper layers of porcine and human skin (stratum corneum, viable epidermis, and dermis – to a total depth 800 μm) following a 12 h application of marketed stick (a) and stick incorporated filters (b) (means ± SD; n = 5 porcine skin, n = 4 human skin; test-t $p < 0.05$). SC = stratum corneum; VE = viable epidermis and DE = dermis.

Table 2
HET-CAM irritancy scores (mean values ± standard deviation; n = 3).

Samples	Concentration (%w/v)	Hemorrhage t (s)	Lysis t (s)	Coagulation t (s)	IS	Classification
SDS	1.0	20	20	0	11.20 ± 0.2	SI
NaOH	1.0	6	6	40	18.74 ± 1.5	SI
NaCl	0.9	0	0	0	0	NI
Stick blank	5.0	0	0	0	0	NI
Stick incorporated filters	5.0	0	0	0	0	NI

Legend: Stick blank with SBA-15; stick incorporated filters; SDS-sodium dodecyl sulfate; IS – irritation index calculated according to Eq. (1); NI – non–irritant; WI – weakly irritant; SI – severely irritant; t = time in seconds.

Indeed, the results presented here showed that incorporated UV filters significantly increased *in vivo* SPF of these compounds. In addition, it was observed that despite a lower content of UVB and UVA filters (OMC, OXY and AVO) in the incorporated stick formulation, it yielded the same photoprotection efficacy as the marketed stick formulation.

4. Conclusions

The present study investigated the efficacy and safety of a stick incorporated filters *in vitro* and *in vivo*. The preclinical and clinical assays proved that SBA-15 and stick filters presented non-irritant and safe profiles. Skin penetration experiments showed that the stick incorporated filters applied to human and porcine skins significantly reduced OXY permeation and cutaneous deposition of OXY and AVO in comparison to the marketed stick product. The biodistribution results demonstrated that encapsulation with SBA-15 decreased the amounts of AVO and OXY present in the deep layers of human and porcine skins (dermis). Comparison between porcine and human skins indicated that the amount of OXY deposited in and permeated across porcine skin was greater than in human skin – most likely due to the presence of terminal hairs in porcine tissue. The *in vivo* assay indicated the SPF values increased by 26% when the UV filters were incorporated into SBA-15. In contrast, UVA-PF results demonstrated that the level of UVA-PF obtained for all formulations were lower than 1/3 of the SPF value. Finally,

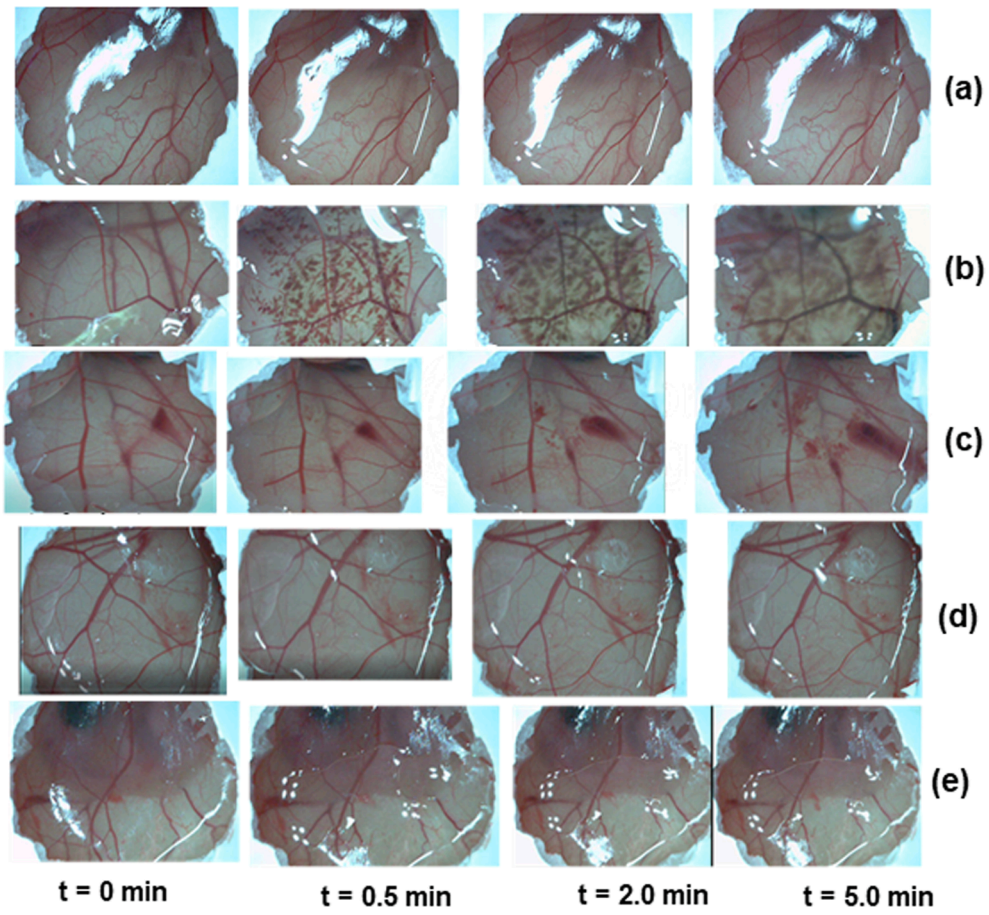

Fig. 7. Images obtained at 0, 0.5 2.0 and 5.0 min of the effect of negative control NaCl solution (a) (1.0% w/v); effects of positive controls NaOH (b) and SDS (c) (1.0% w /v); effects of stick blank/SBA-15 (d) and stick formulation with incorporated filters (e) on the chorioallantoic membrane.

Table 3
Results of clinical safety analysis adapted from Draize Scale.

Clinical Assay	Draize Scale					
	Marketed stick		Stick non-incorporated filters		Stick incorporated filters	
	Erythema	Edema	Erythema	Edema	Erythema	Edema
Primary and accumulated skin irritation	0	0	0	0	0	0
Dermal sensitivity	0	0	0	0	0	0
Photoirritation	0	0	0	0	0	0
Photosensitivity potential	0	0	0	0	0	0

Draize Scale = 0: no erythema or edema.

Table 4
In vitro SPF and critical wavelength (nm) values (mean and standard deviation).

Formulations	In vitro SPF	Critical wavelength (nm)
Marketed stick	142.2 ± 17.3^{B}	374.3 ± 0.6^{D}
Stick incorporated filters	179.3 ± 6.5^{A}	375.0 ± 1.0^{D}
Stick non-incorporated filters	94.3 ± 5.5^{C}	374.6 ± 0.6^{D}

Legend: The results were evaluated according to one-way ANOVA test followed by Tukey test for comparison between samples. Different letters for the same parameter indicate statistically significant differences between samples ($n = 3$; $p < 0.05$); Marketed stick; Stick incorporated filters and Stick non-incorporated filters

the stick incorporated filters yielded the same SPF profile with despite a lower UV filter content than the marketed stick.

Table 5
In vivo SPF and *in vitro* UVA-PF results. Ten volunteers were analysed for SPF test. For the UVA-PF, the results were analysed in quadruplicate.

Formulations	SPF	UVA-PF
Marketed stick	69.5 ± 14.4^{A}	12.9 ± 3.4^{C}
Stick incorporated filters	63.7 ± 10.1^{A}	16.7 ± 2.7^{D}
Stick non-incorporated filters	50.4 ± 10.2^{B}	17.1 ± 2.0^{D}

Legend: Different letters for the same parameter indicate statistically significant differences between samples (SPF *in vivo* ($n = 10$) and UVA-PF ($n = 4$); $p < 0.05$); Marketed stick; Stick incorporated filters and Stick non-incorporated filters.

Declaration of Competing Interest

The authors declare that they have no known competing financial interests or personal relationships that could have appeared to influence the work reported in this paper.

Acknowledgements

The authors would like to acknowledge the financial support of Coordenação de Aperfeiçoamento de Pessoal de Nível Superior (CAPES) and Fundação de Amparo à Pesquisa do Estado de São Paulo (FAPESP, process number 2013/18689-5). This study was financed in part by the Programa de Sanduíche no Exterior (PDSE) from CAPES – Brazil. We would also like to acknowledge University of Geneva and Investiga Research Institute (Alergisa- Campinas – Brazil).

Appendix A. Supplementary material

Supplementary data to this article can be found online at https://doi.org/10.1016/j.ejpb.2021.10.002.

References

[1] L.C. Tomazelli, M.M. de Assis Ramos, R. Sauce, T.M. Cândido, F.D. Sarruf, C.A.S. de Oliveira Pinto, C.A. de Oliveira, C. Rosado, M.V.R. Velasco, A.R. Baby, SPF enhancement provided by rutin in a multifunctional sunscreen, Int. J. Pharm. 552 (1-2) (2018) 401–406, https://doi.org/10.1016/j.ijpharm.2018.10.015.

[2] K. Morabito, N.C. Shapley, K.G. Steeley, A. Tripathi, Review of sunscreen and the emergence of non-conventional absorbers and their applications in ultraviolet protection, Int. J. Cosmet. Sci. 33 (2011) 385–390, https://doi.org/10.1111/j.1468-2494.2011.00654.x.

[3] C. Couteau, M. Pommier, E. Paparis, L.J.M. Coiffard, Study of the efficacy of 18 sun filters authorized in European Union tested in vitro, Pharmazie. 62 (2007) 449–452, https://doi.org/10.1691/ph.2007.6.6247.

[4] E. Gilbert, L. Roussel, C. Serre, R. Sandouk, D. Salmon, P. Kirilov, M. Haftek, F. Falson, F. Pirot, Percutaneous absorption of benzophenone-3 loaded lipid nanoparticles and polymeric nanocapsules: a comparative study, Int. J. Pharm. 504 (1-2) (2016) 48–58, https://doi.org/10.1016/j.ijpharm.2016.03.018.

[5] B. Imamović, M. Šober, E. Bečić, Identification and determination butylmethoxydibenzoylmethane in the presence benzophenone-3 and ethylhexylmethoxycinnamate in suncare preparation, Int. J. Cosmet. Sci. 31 (2009) 383–389, https://doi.org/10.1111/j.1468-2494.2009.00504.x.

[6] M. Wharton, M. Geary, N. O'Connor, B. Murphy, A rapid High Performance Liquid Chromatographic (HPLC) method for the simultaneous determination of seven UV filters found in sunscreen and cosmetics, Int. J. Cosmet. Sci. 33 (2011) 164–170, https://doi.org/10.1111/j.1468-2494.2010.00607.x.

[7] H.J. Leong, I. Jang, K.-S. Hyun, S.-K. Jung, G.-H. Hong, H.-A. Jeong, S.-G. Oh, Preparation of alpha-bisabolol and phenylethyl resorcinol/TiO2 hybrid composites for potential applications in cosmetics, Int. J. Cosmet. Sci. 38 (5) (2016) 524–534, https://doi.org/10.1111/ics.2016.38.issue-510.1111/ics.12339.

[8] A.C. Cozzi, P. Perugini, S. Gourion-arsiquaud, Comparative behavior between sunscreens based on free or encapsulated UV filters in term of skin penetration, retention and photo-stability, Eur. J. Pharm. Sci. 121 (2018) 309–318, https://doi.org/10.1016/j.ejps.2018.06.001.

[9] C. Puglia, E. Damiani, A. Offerta, L. Rizza, G.G. Tirendi, M.S. Tarico, S. Curreri, F. Bonina, R.E. Perrotta, Evaluation of nanostructured lipid carriers (NLC) and nanoemulsions as carriers for UV-filters: characterization, in vitro penetration and photostability studies, Eur. J. Pharm. Sci. 51 (2014) 211–217, https://doi.org/10.1016/j.ejps.2013.09.023.

[10] S. Miksa, D. Lutz, C. Guy, E. Delamour, New approach for a reliable in vitro sun protection factor method – Part II: Practical aspects and implementations, Int. J. Cosmet. Sci. 38 (5) (2016) 504–511, https://doi.org/10.1111/ics.2016.38.issue-510.1111/ics.12327.

[11] P.-S. Wu, L.-N. Huang, Y.-C. Guo, C.-C. Lin, Effects of the novel poly(methyl methacrylate) (PMMA)-encapsulated organic ultraviolet (UV) filters on the UV absorbance and in vitro sun protection factor (SPF), J. Photochem. Photobiol. B Biol. 131 (2014) 24–30, https://doi.org/10.1016/j.jphotobiol.2014.01.006.

[12] G.H.G. Trossini, V.G. Maltarollo, R.D. Garcia, C.A.S.O. Pinto, M.V.R. Velasco, K. M. Honorio, A.R. Baby, Theoretical study of tautomers and photoisomers of avobenzone by DFT methods, J. Mol. Model. 21 (2015) 319, https://doi.org/10.1007/s00894-015-2863-2.

[13] S. Afonso, K. Horita, J.P. Sousa e Silva, I.F. Almeida, M.H. Amaral, P.A. Lobão, P. C. Costa, M.S. Miranda, J.C.G. Esteves da Silva, J.M. Sousa Lobo, Photodegradation of avobenzone: stabilization effect of antioxidants, J. Photochem. Photobiol. B Biol. 140 (2014) 36–40, https://doi.org/10.1016/j.jphotobiol.2014.07.004.

[14] Y.-C. Lin, C.-F. Lin, A. Alalaiwe, P.-W. Wang, Y.-P. Fang, J.-Y. Fang, UV filter entrapment in mesoporous silica hydrogel for skin protection against UVA with minimization of percutaneous absorption, Eur. J. Pharm. Sci. 122 (2018) 185–194, https://doi.org/10.1016/j.ejps.2018.07.013.

[15] S. Tampucci, S. Burgalassi, P. Chetoni, D. Monti, Cutaneous permeation and penetration of sunscreens: formulation strategies and in vitro methods, Cosmetics 5 (2017) 1, https://doi.org/10.3390/cosmetics5010001.

[16] N.R. Janjua, B. Kongshoj, A.-M. Andersson, H.C. Wulf, Sunscreens in human plasma and urine after repeated whole-body topical application, J. Eur. Acad. Dermatol. Venereol. 22 (4) (2008) 456–461, https://doi.org/10.1111/j.1468-3083.2007.02492.x.

[17] C.G.J. Hayden, S.E. Cross, C. Anderson, N.A. Saunders, M.S. Roberts, Sunscreen penetration of human skin and related keratinocyte toxicity after topical application, Skin Pharmacol. Physiol. 18 (4) (2005) 170–174, https://doi.org/10.1159/000085861.

[18] Y. Deng, A. Ediriwickrema, F. Yang, J. Lewis, M. Girardi, W.M. Saltzman, A sunblock based on bioadhesive nanoparticles, Nat. Mater. 14 (12) (2015) 1278–1285, https://doi.org/10.1038/nmat4422.

[19] C.A. De Oliveira, D.D.A. Peres, F. Graziola, N.A.B. Chacra, G.L.B. De Araújo, A. C. Flórido, J. Mota, C. Rosado, M.V.R. Velasco, L.M. Rodrigues, A.S. Fernandes, A. R. Baby, Cutaneous biocompatible rutin-loaded gelatin-based nanoparticles increase the SPF of the association of UVA and UVB filters, Eur. J. Pharm. Sci. 81 (2016) 1–9, https://doi.org/10.1016/j.ejps.2015.09.016.

[20] S.A. Wissing, R.H. Müller, Solid lipid nanoparticles as carrier for sunscreens: in vitro release and in vivo skin penetration, J. Control. Release 81 (3) (2002) 225–233, https://doi.org/10.1016/S0168-3659(02)00056-1.

[21] S.G. Kandekar, S. del Río-Sancho, M. Lapteva, Y.N. Kalia, Selective delivery of adapalene to the human hair follicle under finite dose conditions using polymeric micelle nanocarriers, Nanoscale 10 (3) (2018) 1099–1110, https://doi.org/10.1039/C7NR07706H.

[22] M. Lapteva, M. Möller, R. Gurny, Y.N. Kalia, Self-assembled polymeric nanocarriers for the targeted delivery of retinoic acid to the hair follicle, Nanoscale 7 (44) (2015) 18651–18662, https://doi.org/10.1039/C5NR04770F.

[23] C.A. de Oliveira, M.F. Dario, F.D. Sarruf, I.F.A. Mariz, M.V.R. Velasco, C. Rosado, A.R. Baby, Safety and efficacy evaluation of gelatin-based nanoparticles associated with UV filters, Colloids Surfaces B Biointerfaces 140 (2016) 531–537, https://doi.org/10.1016/j.colsurfb.2015.11.031.

[24] F. Larese Filon, M. Mauro, G. Adami, M. Bovenzi, M. Crosera, Nanoparticles skin absorption: new aspects for a safety profile evaluation, Regul. Toxicol. Pharmacol. 72 (2) (2015) 310–322, https://doi.org/10.1016/j.yrtph.2015.05.005.

[25] M. Roberts, Y. Mohammed, M. Pastore, S. Namjoshi, S. Yousef, A. Alinaghi, I. Haridass, E. Abd, V. Leite-Silva, H. Benson, J. Grice, Topical and cutaneous delivery using nanosystems, J. Control. Release 247 (2017) 86–105, https://doi.org/10.1016/j.jconrel.2016.12.022.

[26] A.L.M. Daneluti, F.M. Neto, M.V.R. Velasco, A.R. Baby, J. do Rosário Matos, Evaluation and characterization of the encapsulation/entrapping process of octyl methoxycinnamate in ordered mesoporous silica type SBA-15, J. Therm. Anal. Calorim. 131 (2018) 789–798, https://doi.org/10.1007/s10973-017-6265-9.

[27] F. Mariano-Neto, J.R. Matos, L.C. Cides da Silva, L.V. Carvalho, K. Scaramuzzi, O. A. Sant'Anna, C.P. Oliveira, M.C.A. Fantini, Physical properties of ordered mesoporous SBA-15 silica as immunological adjuvant, J. Phys. D. Appl. Phys. 47 (42) (2014) 425402, https://doi.org/10.1088/0022-3727/47/42/425402.

[28] S.G. de Ávila, L.C.C. Silva, J.R. Matos, Optimisation of SBA-15 properties using Soxhlet solvent extraction for template removal, Microporous Mesoporous Mater. 234 (2016) 277–286, https://doi.org/10.1016/j.micromeso.2016.07.027.

[29] H.S. Neto, G.L.B. de Araujo, L.L. dos Santos, I.C. Cosentino, F.M. de Souza Carvalho, J. do Rosário Matos, Inclusion of prednicarbate in the SBA-15 silica, J. Therm. Anal. Calorim. 123 (2016) 2297–2305, https://doi.org/10.1007/s10973-015-4945-x.

[30] J.R. Matos, L.P. Mercuri, M. Kruk, M. Jaroniec, Toward the synthesis of extra-large-pore MCM-41 analogues, Chem. Mater. 13 (5) (2001) 1726–1731, https://doi.org/10.1021/cm000964p.

[31] Y. Zhou, G. Quan, Q. Wu, X. Zhang, B. Niu, B. Wu, Y. Huang, X. Pan, C. Wu, Mesoporous silica nanoparticles for drug and gene delivery, Acta Pharm. Sin. B. 8 (2) (2018) 165–177, https://doi.org/10.1016/j.apsb:2018.01.007.

[32] U. Ciesla, F. Schüth, Ordered mesoporous materials, Microporous Mesoporous Mater. 27 (2-3) (1999) 131–149, https://doi.org/10.1016/S1387-1811(98)00249-2.

[33] M. Al Shamsi, M.T. Al Samri, S. Al-Salam, W. Conca, S. Shaban, S. Benedict, S. Tariq, A.V. Biradar, H.S. Penefsky, T. Asefa, A.-K. Souid, Biocompatibility of calcined mesoporous silica particles with cellular bioenergetics in murine tissues, Chem. Res. Toxicol. 23 (11) (2010) 1796–1805, https://doi.org/10.1021/tx100245j.

[34] T. López, E.I. Basaldella, M.L. Ojeda, J. Manjarrez, R. Alexander-Katz, Encapsulation of valproic acid and sodic phenytoin in ordered mesoporous SiO2 solids for the treatment of temporal lobe epilepsy, Opt. Mater. (Amst) 29 (1) (2006) 75–81, https://doi.org/10.1016/j.optmat.2006.03.017.

[35] S.P. Hudson, R.F. Padera, R. Langer, D.S. Kohane, The biocompatibility of mesoporous silicates, Biomaterials 29 (30) (2008) 4045–4055, https://doi.org/10.1016/j.biomaterials.2008.07.007.

[36] C.-Y. Lai, B.G. Trewyn, D.M. Jeftinija, K. Jeftinija, S. Xu, S. Jeftinija, V.-Y. Lin, A mesoporous silica nanosphere-based carrier system with chemically removable CdS nanoparticle caps for stimuli-responsive controlled release of neurotransmitters and drug molecules, J. Am. Chem. Soc. 125 (15) (2003) 4451–4459, https://doi.org/10.1021/ja028650l.

[37] A.L.M. Daneluti, F.M. Neto, N. Ruscinc, I. Lopes, M.V. Robles Velasco, J. Do Rosário Matos, A.R. Baby, Y.N. Kalia, Using ordered mesoporous silica SBA-15 to limit cutaneous penetration and transdermal permeation of organic UV filters, Int. J. Pharm. 570 (2019) 118633, https://doi.org/10.1016/j.ijpharm.2019.118633.

[38] L.R. Gaspar, P.M.B.G. Maia Campos, Evaluation of the photostability of different UV filter combinations in a sunscreen, Int. J. Pharm. 307 (2) (2006) 123–128, https://doi.org/10.1016/j.ijpharm.2005.08.029.

[39] L.M. Peruchi, S. Rath, Development and application of a HPLC method for eight sunscreen agents in suncare products, Int. J. Cosmet. Sci. 34 (2012) 226–233, https://doi.org/10.1111/j.1468-2494.2012.00703.x.

[40] A. Salvador, M.D. de la Ossa, A. Chisvert, Determination of butyl methoxydibenzoylmethane, benzophenone-3, octyl dimethyl PABA and octyl

methoxycinnamate in lipsticks, Int. J. Cosmet. Sci. 25 (3) (2003) 97–102, https://doi.org/10.1046/j.1467-2494.2003.00178.x.
[41] M. Lapteva, M. Mignot, K. Mondon, M. Möller, R. Gurny, Y.N. Kalia, Self-assembled mPEG-hexPLA polymeric nanocarriers for the targeted cutaneous delivery of imiquimod, Eur. J. Pharm. Biopharm. 142 (2019) 553–562, https://doi.org/10.1016/j.ejpb.2019.01.008.
[42] National Institute of Environmental Health Sciences (NIEHS), ICCVAM TEST METHOD EVALUATION REPORT: In vitro Ocular Toxicity Test Methods for Identifying Severe Irritants and Corrosives, NIH Publication, 2010.
[43] T.D. Wilson, W.F. Steck, A modified HET–CAM assay approach to the assessment of anti-irritant properties of plant extracts, Food Chem. Toxicol. 38 (10) (2000) 867–872, https://doi.org/10.1016/S0278-6915(00)00091-0.
[44] M.F. Dario, C.A. Oliveira, L.R.G. Cordeiro, C. Rosado, I. de F.A. Mariz, E. Maçôas, M.S.C.S. Santos, M.E. Minas da Piedade, A.R. Baby, M.V.R. Velasco, Stability and safety of quercetin-loaded cationic nanoemulsion: In vitro and in vivo assessments, Colloids Surfaces A Physicochem. Eng. Asp. 506 (2016) 591–599, https://doi.org/10.1016/j.colsurfa.2016.07.010.
[45] S. Kalweit, R. Besoke, I. Gerner, H. Spielmann, A national validation project of alternative methods to the Draize rabbit eye test, Toxicol. Vitr. 4 (4-5) (1990) 702–706, https://doi.org/10.1016/0887-2333(90)90147-L.
[46] D. Jírová, D. Basketter, M. Liebsch, H. Bendová, K. Kejlová, M. Marriott, H. Kandárová, Comparison of human skin irritation patch test data with in vitro skin irritation assays and animal data, Contact Dermatitis. 62 (2010) 109–116, https://doi.org/10.1111/j.1600-0536.2009.01640.x.
[47] A.M. Kligman, W.M. Wooding, A method for the measurement and evaluation of irritants on human skin, J. Invest. Dermatol. 49 (1967) 78–94, https://doi.org/10.1038/jid.1967.106.
[48] D.D.A. Peres, F.D. Sarruf, C.A. de Oliveira, M.V.R. Velasco, A.R. Baby, Ferulic acid photoprotective properties in association with UV filters: multifunctional sunscreen with improved SPF and UVA-PF, J. Photochem. Photobiol. B Biol. 185 (2018) 46–49, https://doi.org/10.1016/j.jphotobiol.2018.05.026.
[49] A.P. Walker, D.A. Basketter, M. Baverel, W. Diembeck, W. Matthies, D. Mougin, M. Paye, R. Röthlisberger, J. Dupuis, Test guidelines for assessment of skin compatibility of cosmetic finished products in man, Food Chem. Toxicol. 34 (7) (1996) 651–660, https://doi.org/10.1016/0278-6915(96)00029-4.
[50] Cosmetics Europe, Guidelines for the safety assessment of a cosmetic product, 2004.
[51] C.W. Stott, J. Stasse, R. Bonomo, A.H. Campbell, Evaluation of the phototoxic potential of topically applied agents using long-wave ultraviolet light from the Johnson & Johnson Research Foundation, New Brunswick, New Jersey, J. Invest. Dermatol. 55 (5) (1970) 335–338, https://doi.org/10.1111/1523-1747.ep12260208.
[52] COLIPA, Methods for testing efficacy of sunscreen products, 2006.
[53] Cosmetic Europe, COLIPA Guidelines. In vitro method for the determination of the UVA protection factor and "'critical wavelength"' values of sunscreen products, 2011.
[54] U. Jacobi, M. Kaiser, R. Toll, S. Mangelsdorf, H. Audring, N. Otberg, W. Sterry, J. Lademann, Porcine ear skin: an in vitro model for human skin, Ski. Res. Technol. 13 (1) (2007) 19–24, https://doi.org/10.1111/srt.2007.13.issue-110.1111/j.1600-0846.2006.00179.x.
[55] P.D. Marcato, J. Caverzan, B. Rossi-Bergmann, E.F. Pinto, D. Machado, R.A. Silva, G.Z. Justo, C.V. Ferreira, N. Durán, Nanostructured polymer and lipid carriers for sunscreen. Biological effects and skin permeation, J. Nanosci. Nanotechnol. 11 (2011) 1880–1886, https://doi.org/10.1166/jnn.2010.3135.
[56] Z. Klimová, J. Hojerová, M. Beránková, Skin absorption and human exposure estimation of three widely discussed UV filters in sunscreens - Invitro study mimicking real-life consumer habits, Food Chem. Toxicol. 83 (2015) 237–250, https://doi.org/10.1016/j.fct.2015.06.025.
[57] M. Lapteva, K. Mondon, M. Möller, R. Gurny, Y.N. Kalia, Polymeric micelle nanocarriers for the cutaneous delivery of tacrolimus: a targeted approach for the treatment of psoriasis, Mol. Pharm. 11 (9) (2014) 2989–3001, https://doi.org/10.1021/mp400639e.
[58] C. Fernandez, G. Marti-mestres, J. Ramos, H. Maillols, LC analysis of benzophenone-3: II application to determination of ' in vitro ' and ' in vivo ' skin penetration from solvents, coarse and submicron emulsions, J. Pharm. Biomed. Anal. 24 (2000) 155–165.
[59] A. Vogt, S. Hadam, M. Heiderhoff, H. Audring, J. Lademann, W. Sterry, U. Blume-Peytavi, Morphometry of human terminal and vellus hair follicles, Exp. Dermatol. 16 (11) (2007) 946–950, https://doi.org/10.1111/exd.2007.16.issue-1110.1111/j.1600-0625.2007.00602.x.
[60] H.-J. Weigmann, S. Schanzer, A. Patzelt, V. Bahaban, F. Durat, W. Sterry, J. Lademann, Comparison of human and porcine skin for characterization of sunscreens, J. Biomed. Opt. 14 (2) (2009) 024027, https://doi.org/10.1117/1.3103340.
[61] J. Marto, A. Ascenso, L.M. Gonçalves, L.F. Gouveia, P. Manteigas, P. Pinto, E. Oliveira, A.J. Almeida, H.M. Ribeiro, Melatonin-based pickering emulsion for skin's photoprotection, Drug Deliv. 23 (5) (2016) 1594–1607, https://doi.org/10.3109/10717544.2015.1128496.
[62] L. Durand, N. Habran, V. Henschel, K. Amighi, In vitro evaluation of the cutaneous penetration of sprayable sunscreen emulsions with high concentrations of UV filters, Int. J. Cosmet. Sci. 31 (2009) 279–292, https://doi.org/10.1111/j.1468-2494.2009.00498.x.
[63] A. Verma, Transfollicular drug delivery: current perspectives, Res. Rep. Transdermal Drug Deliv. (2016) 1–17.
[64] J. Lademann, U. Jacobi, C. Surber, H.-J. Weigmann, J.W. Fluhr, The tape stripping procedure – evaluation of some critical parameters, Eur. J. Pharm. Biopharm. 72 (2) (2009) 317–323, https://doi.org/10.1016/j.ejpb.2008.08.008.
[65] H. Abdelkader, B. Pierscionek, M. Carew, Z. Wu, R.G. Alany, Critical appraisal of alternative irritation models: three decades of testing ophthalmic pharmaceuticals, Br. Med. Bull. 113 (1) (2015) 59–71, https://doi.org/10.1093/bmb/ldv002.
[66] N.P. Luepke, F.H. Kemper, The HET-CAM test: an alternative to the draize eye test, Food Chem. Toxicol. 24 (6-7) (1986) 495–496, https://doi.org/10.1016/0278-6915(86)90099-2.
[67] W. Steiling, M. Bracher, P. Courtellemont, O. de Silva, The HET-CAM, a useful in vitro assay for assessing the eye irritation properties of cosmetic formulations and ingredients, Toxicol. Vitr. 13 (2) (1999) 375–384, https://doi.org/10.1016/S0887-2333(98)00091-5.
[68] T.D. Wilson, W.F. Steck, Research Section A modified HET ± CAM assay approach to the assessment of anti-irritant properties of plant extracts, Food Chem. Toxicol. 38 (10) (2000) 867–872.
[69] FDA, Guidance Documents – Guidance for Industry: Safety of Nanomaterials in Cosmetic Products, 2012, pp. 1–16.
[70] C.T. Kresge, M.E. Leonowicz, W.J. Roth, J.C. Vartuli, J.S. Beck, Ordered mesoporous molecular sieves synthesized by a liquid-crystal template mechanism, Nature 359 (6397) (1992) 710–712, https://doi.org/10.1038/359710a0.
[71] Y. Choi, J.E. Lee, J.H. Lee, J.H. Jeong, J. Kim, A biodegradation study of SBA-15 microparticles in simulated body fluid and in vivo, Langmuir 31 (23) (2015) 6457–6462, https://doi.org/10.1021/acs.langmuir.5b01316.
[72] D. Moyal, How to measure UVA protection afforded by sunscreen products, Expert Rev. Dermatol. 3 (3) (2008) 307–313, https://doi.org/10.1586/17469872.3.3.307.
[73] M. Pelizzo, E. Zattra, P. Nicolosi, A. Peserico, D. Garoli, M. Alaibac, In vitro evaluation of sunscreens: an update for the clinicians, ISRN Dermatol. 2012 (2012) 1–4, https://doi.org/10.5402/2012/352135.
[74] J.P. Santos Caetano, A.P. Abarca, M. Guerato, L. Guerra, S. Schalka, D.C. Perez Simão, R. Vila, SPF and UVA-PF sunscreen evaluation: are there good correlations among results obtained in vivo, in vitro and in a theoretical Sunscreen Simulator? A real-life exercise, Int. J. Cosmet. Sci. 38 (6) (2016) 576–580, https://doi.org/10.1111/ics.2016.38.issue-610.1111/ics.12322.
[75] J.F. Nash, P.R. Tanner, Relevance of UV filter/sunscreen product photostability to human safety, Photodermatol. Photoimmunol. Photomed. 30 (2-3) (2014) 88–95, https://doi.org/10.1111/phpp.2014.30.issue-2-310.1111/phpp.12113.
[76] M.S. Frizzo, P.E. Feuser, P.H. Berres, E. Ricci-Júnior, C.E.M. Campos, C. Costa, P.H. H. de Araújo, C. Sayer, Simultaneous encapsulation of zinc oxide and octocrylene in poly (methyl methacrylate-co-styrene) nanoparticles obtained by miniemulsion polymerization for use in sunscreen formulations, Colloids Surfaces A Physicochem. Eng. Asp. 561 (2019) 39–46, https://doi.org/10.1016/j.colsurfa.2018.10.062.
[77] S. Scalia, S. Battaglioli, A. Bianchi, In vivo human skin penetration of the UV filter ethylhexyl triazone: effect of lipid microparticle encapsulation, Skin Pharmacol. Physiol. 32 (1) (2018) 22–31, https://doi.org/10.1159/000493761.